JOURNAL OF THEORETICAL
AND APPLIED MECHANICS
64, 2, pp. 131–144, Warsaw 2026
https://doi.org/10.15632/jtam-pl/221438

DRIVING TORQUE FOR A STEER-BY-WIRE SYSTEM HAND WHEEL ACTUATOR BASED ON THE REFERENCE DRIVING TORQUE FROM AN ELECTRIC POWER STEERING SYSTEM

Marek Bogdan BRYKCZYŃSKI*, Andrzej HARLECKI

Faculty of Mechanical Engineering and Computer Science, University of Bielsko-Biała, Bielsko-Biała, Poland
*corresponding author, *marek.brykczynski@gmail.com*

This paper experimentally determines an electric motor driving torque for a steer-by-wire (SBW) system hand wheel actuator (HWA). An equivalent electric motor driving torque for an SBW system HWA is determined with an objective to mirror the steering wheel angular position trajectory of an electric power steering (EPS) system by iterative examination of steering wheel trajectories of the SBW system HWA obtained for a series of driving torques against those from a reference EPS. The objective function criteria are defined by a maximum value of a mean relative error of the steering wheel angular position.

Keywords: driving torque; electric power steering; hand wheel actuator; road wheel actuator; steer-by-wire.

Articles in JTAM are published under Creative Commons Attribution 4.0 International.
Unported License https://creativecommons.org/licenses/by/4.0/deed.en.
By submitting an article for publication, the authors consent to the grant of the said license.

Nomenclature

Constant parameters

c_{em}, $c_{em'}$, $c_{em''}$ – viscous damping coefficient of the EPS motor, HWA motor, and RWA motor [Nm · s],
c_{ms}, $c_{ms'}$, $c_{ms''}$ – viscous damping coefficient of the electric motor shaft and worm engagement for: EPS system, HWA and RWA [Nm · s],
$c_r, c_{r''}$ – damping coefficient of the steering rack for EPS and RWA [Ns/m],
c_{sw}, $c_{sw'}$ – viscous damping coefficient of the EPS steering wheel and HWA steering wheel [Nms],
k_{ms}, $k_{ms'}$, $k_{ms''}$ – stiffness coefficient of the electric motor shaft engagements with a worm gear [Nm/rad],
k_r, $k_{r''}$ – stiffness coefficient of the steering rack for EPS and RWA [N/m],
k_{tb}, $k_{tb'}$ – stiffness coefficient of the torsion bars of the EPS and HWA [Nm/rad],
m_r, $m_{r''}$ – mass of the steering rack of the EPS and RWA [kg],
m_{wg}, m_{ww} – mass of the worm and worm wheel [kg],
r_p – radius of the pinion transmitting power to the rack [m],
C_f – C-factor – coefficient describing the linear displacement of the rack relative to the angular displacement of the pinion [mm/rad],
J_{em}, $J_{em'}$, $J_{em''}$ – moments of inertia of electric motors for: EPS, HWA, and RWA [kg · m^2],
J_{sw}, $J_{sw'}$ – moments of inertia of the EPS steering wheel and HWA steering wheel [kg · m^2],
J_{wg}, $J_{wg'}$, $J_{wg''}$ – symbols of the moment of inertia of the worm gear in: EPS, HWA, and RWA [kg · m^2],
J_{ww}, $J_{ww'}$, $J_{ww''}$ – symbols of the moment of inertia of the column and worm wheel assembly in: EPS, HWA, and RWA [kg · m^2],
$T_{\max} = 4.5$ – value of the maximum driving torque on the electric motor shaft [Nm] (Nidec Corporation, n.d.),
$\tau = 125$ – duration of the pulse shaped driving torque excitation [ms],
τ_{HWA} – time constant of the analyzed HWA model for the transfer function $\theta_{sw'} = \theta_{sw'}(T_{em'})$.

Input signals:

F_r – a value of rack force interacting on tie rods [N],
T_{em}, $T_{em'}$, $T_{em''}$ – values of driving torques generated by the EPS motor, HWA motor, and RWA motor [Nm],
T^a_{em} – a value of a reference driving torque from the EPS system [Nm],

$T^b_{em'}(j)$ – a value of a j-index driving torque for the HWA subsystem [Nm],
T_{dr} – a value of a driver's torque (external torque on the steering wheel) [Nm].

Variables:

θ_{em}, $\theta_{em'}$, $\theta_{em''}$ – angular displacements of the electric motor shaft for: EPS, HWA, and RWA [rad],
θ_{sw}, $\theta_{sw'}$ – sequentially angular displacements of the steering wheel for EPS and HWA [rad],
θ_{wg}, $\theta_{wg'}$, $\theta_{wg''}$ – sequentially worm gear angular displacements of the EPS, HWA, and RWA [rad],
θ_{ww}, $\theta_{ww'}$, $\theta_{ww''}$ – sequentially worm wheel angular displacements of the EPS, HWA, and RWA [rad],
χ_r, $\chi_{r''}$ – linear displacement of the steering rack for EPS and RWA [m],
$T_{cww} = T_{cww}(\theta_{wg}, \theta_{ww})$, $T_{cwg} = T_{cwg}(\theta_{wg}, \theta_{ww}), T_{cww'}, T_{cwg'}, T_{cww''}, T_{cwg''}$ – the reaction torques of the worm wheel and the worm gear in a worm drive [Nm].

1. Introduction

The steering system is responsible for positioning the vehicle's front (steered) wheels at the correct angle and, consequently, for controlling the desired direction of driving (steering). It "transmits" commands from the driver to steering knuckles, and simultaneously, in the opposite direction, "transmits" information to the driver about the vehicle current position on the road, also "allowing" the driver to sense the torque (torque of resistance) exerted on the steering wheel by the steering system, which is the result of the road's resistance forces acting on the front wheels. The coming years are expected to see a radical shift in the way automotive steering systems operate. It is predicted that the conventional electric power steering (EPS) systems currently used in (passenger) vehicles, in which the steering wheel is mechanically connected to the steering knuckles via the steering column, will in the future be replaced by steer-by-wire (SBW) systems. In these systems, the steering wheel and steering knuckles are connected solely via an electrical interface (an electrical communication bus), eliminating the mechanical connection.

The aim of the research described in this article is to determine the electric motor driving torque for the SBW system hand wheel actuator (HWA) subsystem, based on the steering wheel angle trajectory from a reference EPS system. As part of the study, the authors implemented a mathematical model of the EPS system and developed a mathematical model for the SBW system. The main focus of this work has been on the HWA subsystem, as both systems are coupled with the steering wheel. The SBW system road wheel actuator (RWA) subsystem is presented for reference to indicate the complete mechanical SBW system model. In the last stage of the study, the authors formulate a functional relation for an electric motor driving torque for the HWA dependent on the reference torque from the EPS system. The resultant function to derive the driving torque from the reference torque is formed with the objective to enable its implementation in the electronic control unit (ECU) of the SBW system, which is a real-time embedded microprocessor system. Consequently, a driver holding the steering wheel of a car equipped with this system will experience steering resistance comparable to an EPS system, resulting from the forces exerted by the road surface on the front wheels. It is worth noting that the EPS system has a significant limitation: the steering ratio between the steering wheel and the steering knuckles remains constant. This limitation is eliminated by the SBW system, which varies the ratio, thus enabling faster turning maneuvers. This, in turn, can significantly aid the driver while parking, as it will require fewer steering wheel turns than with a conventional EPS system.

After the introduction, the authors review available literature, starting with EPS systems, then followed by SBW systems. In the next step, the mathematical models of the EPS system and SBW system are presented and followed by the model comparison with the indication of key mechanical differences. Subsequently, the authors present the objective, methodology and results of their research. Finally, conclusions are drawn, indicating a direction for further research.

2. Literature review

The first scientific paper introducing an EPS system in (passenger) vehicles was published by Shimizu and Kawai (1991), where the authors presented the EPS system concept along with basic

research on such a solution and its impact on reducing fuel consumption by 5.5 % compared to an electrohydraulic power steering system. Badawy *et al.* (1999) devised a modeling strategy for the EPS system and its transformation into a simplified model aimed at providing basic criteria for automatic steering systems. Canudas-de-Wit *et al.* (2005) focused on a review of automatic steering techniques to improve driving comfort while ensuring satisfactory functional safety for EPS systems. Research results by Pfeffer *et al.* (2008) described the effect of changes in the main parameters of the EPS system on steering torque, steering feel, and vehicle understeer. A model for an EPS system that integrates a control algorithm for basic assistance functionality, damping, steering return, and inertia compensation was proposed by Hu *et al.* (2008). Chen *et al.* (2011) presented a model of the EPS system and a method for developing a boost curve incorporated into the power steering characteristics to improve the mobility and stability of a steering system equipped with EPS. In their research, Ciarla *et al.* (2012) conducted a study of amplification criteria in boost curves, including steering wheel jerk and friction phenomena in the EPS system. Tamura *et al.* (2013) proposed a model incorporating the LuGre friction model for a column-type EPS system to analyze its performance under static and dynamic operating conditions. A method for active friction compensation in a column-type EPS system was presented by Wilhelm *et al.* (2016). In this study, a model of a column EPS system was proposed that takes into account the influence of slip and pressure on friction forces. Mirmohammad Sadeghi *et al.* (2017) established a procedure for determining friction forces for a column-type EPS system. Kuranowski (2019) published a dynamic model of the EPS system along with the results of its correlation with the tested real system, which demonstrated good model correlation with the real system. Manca *et al.* (2021) conducted research to estimate the performance of the EPS system for an autonomous, fully electric, four-wheel drive racing car participating in the Formula Student competition. Jang *et al.* (2022) proposed a method for modeling the torque from the road forces acting on the EPS system. Haas *et al.* (2023) developed a method for objectively evaluating feedback from a steering system equipped with an EPS system to the driver, which affects functional safety. Guan *et al.* (2024) formulated a closed-loop automatic control strategy for the EPS system, oriented towards steering wheel feel. Nguyen (2025) conducted a review of the scientific literature, classifying and analyzing various types of characteristics of EPS system assistance curves.

SBW systems are an evolution of EPS-based vehicle control. SBW technology is part of the X-By-Wire (XBW) family of technical solutions, of which the first production-scale implementation started with the Fly-By-Wire system in the F-16 Fighting Falcon military aircraft in 1973. In 1988, Fly-By-Wire technology was implemented in the Airbus A320 commercial passenger aircraft, which entered service with Air France. The first example of a car without a conventional mechanical coupling between the steering wheel and the steering rack was the Saab Prometheus concept car, presented in 1992. The vehicle was controlled using a joystick. Due to the difficulties of driving, the concept was not further developed. In 1996, Mercedes-Benz introduced the Mercedes-Benz F200 Imagination in Paris, in which the vehicle control system was implemented using two joysticks. The first scientific publications on SBW systems in the automotive industry date back to 1999, when Führer and Schedl (1999) presented research results demonstrating enormous potential for increasing passive and active functional safety in motor vehicles. Dilger *et al.* (1999) obtained a patent in the United States for a technical solution for the steering wheel control (steer-by-wire) steering system. Feick *et al.* (2000) published research results on a redundant steering wheel control (steer-by-wire) system providing force feedback to the driver on the vehicle's interaction with the road while driving. Dominke *et al.* (2002) published a patent proposing a strategy for increasing the level of functional safety in the steering wheel control (steer-by-wire) system through the use of auxiliary diagnostics of key signals. In the following years, further patents were published on various technical solutions for the HWA subsystem by Magnus *et al.* (2002) and Menjak *et al.* (2004). Yih and Gerdes (2004) published research conducted on a vehicle with an SBW system, which included an estimation

of its side slip angle using information about the steering torque. Li and He (2005) proposed a bond graph model of the SBW system and conducted simulations of the dynamic behavior of the system in terms of the vehicle's maneuverability and steering feel. Yih (2005) presented doctoral thesis research on the impact of the SBW system on interaction with the car and on functional safety. Kazemi and Mousavinejad (2011) devised a new method of modeling the SBW system by applying the bond graph theory. Han *et al.* (2014) developed a method for designing the torque ratio based on the characteristics of the torque on the steering wheel in the SBW system. Tavoosi *et al.* (2014) presented a control algorithm aimed at improving the controllability of a car with an SBW system. In their work, they used a four-degree-of-freedom model and tested it in a hardware in the loop (HIL) environment. Polmans (2016) published a patent introducing a technical solution for the SBW system in which each front wheel had a separate RWA positioning system. Eickholt *et al.* (2019) published a patent presenting the mechanical assembly of the RWA subsystem components. Yin *et al.* (2024) formulated a control algorithm for the SBW system using a two-layer closed-loop model. The study proposed a strategy for observing the difference in the steering angle of the wheels in order to achieve a given steering angle. Perdana *et al.* (2025) conducted studies on various control strategies for SBW systems, assessing their impact on individual goals set for automatic control algorithms, such as: accuracy of obtained output values, operating range, feedback from the control system, and error detection.

The analyzed literature addresses either EPS or SBW systems separately, investigating their modeling, advanced control algorithms, and interaction with the vehicle. The present study focuses on providing methodology for determining the driving torque of the electric motor in the hand wheel actuator (HWA) of a steer-by-wire (SBW) system, using the driving torque characteristics of an electronic motor employed in a conventional electric power steering (EPS) system as the reference basis. The research aims to reproduce the steering wheel dynamics of the conventional EPS system, thereby ensuring that the driver experiences a comparable steering sensation.

3. Mathematical models

3.1. Conventional EPS system

The primary part of the column EPS system in Fig. 1 is the column (1), which is connected at the top to the steering wheel via a torsion bar (2). The lower end of the column is connected via a universal joint (3) to the upper end of the intermediate shaft (4). The lower end of this shaft is connected by means of another universal joint (3) with the upper end of the output shaft (5), which, at its lower end, has a pinion (6), cooperating with a toothed bar (7). The column-type

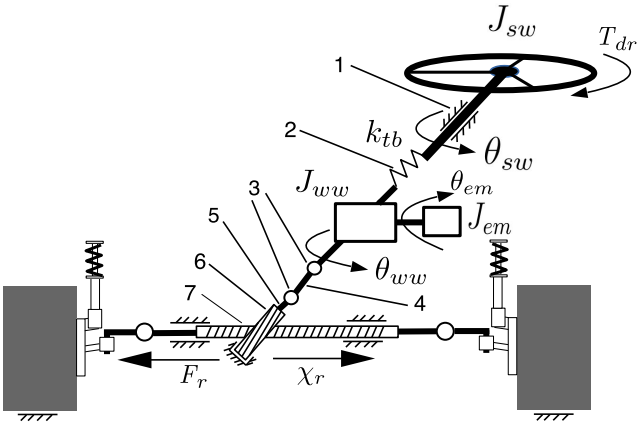

Fig. 1. Conventional EPS system with a column.

EPS system can be represented by the following equations of motion as shown by Hu *et al.* (2008) and later Tamura *et al.* (2013):

$$J_{sw}\ddot{\theta}_{sw} = -k_{tb}(\theta_{sw} - \theta_{ww}) - c_{sw}\dot{\theta}_{sw} + T_{dr}, \tag{3.1}$$

$$J_{ww}\ddot{\theta}_{ww} = k_{tb}(\theta_{sw} - \theta_{ww}) - r_p C_f k_r \left(\theta_{ww} - \frac{\chi_r}{C_f}\right) - c_{ww}\dot{\theta}_{ww} + T_{cww}, \tag{3.2}$$

$$J_{wg}\ddot{\theta}_{wg} = k_{ms}(\theta_{em} - \theta_{wg}) + c_{ms}(\dot{\theta}_{em} - \dot{\theta}_{wg}) + T_{cwg}, \tag{3.3}$$

$$J_{em}\ddot{\theta}_{em} = T_{em} - k_{ms}(\theta_{em} - \theta_{wg}) - c_{ms}(\dot{\theta}_{em} - \dot{\theta}_{wg}) - c_{em}\dot{\theta}_{em}, \tag{3.4}$$

$$m_r\ddot{\chi}_r = k_r(C_f\theta_{ww} - \chi_r) - c_r\dot{\chi}_r - F_r. \tag{3.5}$$

3.2. SBW steering system

The SBW steering system shown in Fig. 2 consists of two subsystems: the HWA and the RWA. The HWA steering subsystem is coupled to the steering wheel. Its main function, as that of the EPS system, is to "read" the driver's commands regarding the desired vehicle direction and, conversely, to "transmit" information to the driver about the current position of the front wheels. Both systems simultaneously "allow" the driver to sense the torque exerted on the steering wheel by the steering system, which is the result of the resistance forces acting on the front wheels from the road. The RWA vehicle wheels positioning subsystem is coupled to the front wheels via a rack and a pinion. The front wheel control unit $\mathrm{ECU_{RWA}}$ adjusts the wheels so that the vehicle can move in the direction specified by the driver. The RWA electronic control unit $\mathrm{ECU_{RWA}}$ microprocessor receives the information (command) about the desired steering direction digitally via a serial communication bus from the $\mathrm{ECU_{HWA}}$ control unit's microprocessor. The coupling digital communication bus between the HWA and the RWA of the SBW system depends on the actual design and can be realized by CAN 2.0, CAN FD, FlexRay or Automotive Ethernet protocols. The mechanical components of an SBW steering system (communication bus-coupled vehicle control system) can be represented by the following equations of motion as published by Han *et al.* (2014) with additional considerations as presented by Tamura *et al.* (2013) and Wilhelm *et al.* (2016).

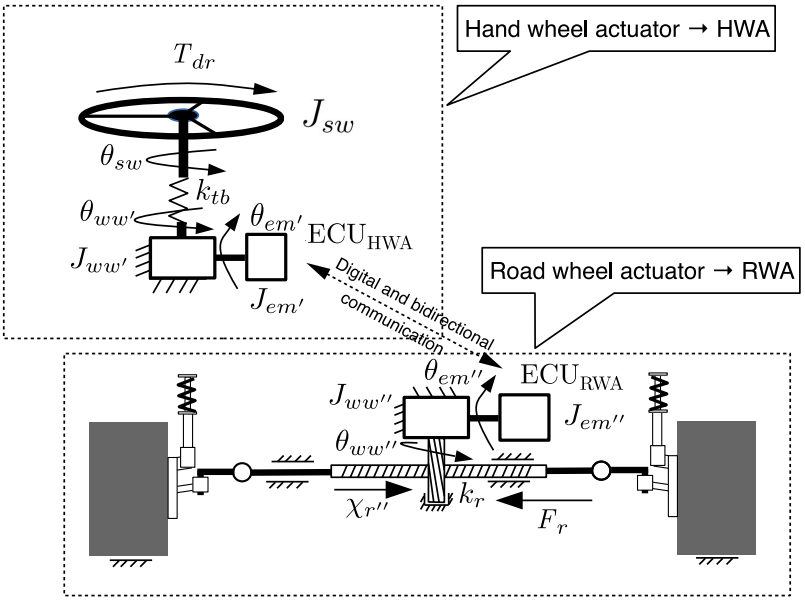

Fig. 2. SBW steering system.

HWA subsystem:

$$J_{sw'}\ddot{\theta}_{sw} = -k_{tb'}(\theta_{sw'} - \theta_{ww'}) - c_{sw'}\dot{\theta}_{sw'} + T_{dr}, \tag{3.6}$$

$$J_{ww'}\ddot{\theta}_{ww'} = k_{tb'}(\theta_{sw'} - \theta_{ww'}) - c_{ww'}\dot{\theta}_{ww'} + T_{cww'}, \tag{3.7}$$

$$J_{wg'}\ddot{\theta}_{wg'} = k_{ms'}(\theta_{em'} - \theta_{wg'}) + c_{ms'}(\dot{\theta}_{em'} - \dot{\theta}_{wg'}) + T_{cwg'}, \tag{3.8}$$

$$J_{em'}\ddot{\theta}_{em'} = T_{em'} - k_{ms'}(\theta_{em'} - \theta_{wg'}) - c_{ms'}(\dot{\theta}_{em'} - \dot{\theta}_{wg'}) - c_{em'}\dot{\theta}_{em'}. \tag{3.9}$$

RWA subsystem:

$$J_{ww''}\ddot{\theta}_{ww''} = -r_p C_f k_{r''}\left(\theta_{ww''} - \frac{\chi_{r''}}{C_f}\right) - c_{ww''}\dot{\theta}_{ww''} + T_{cww''}, \tag{3.10}$$

$$J_{wg''}\ddot{\theta}_{wg''} = k_{ms''}(\theta_{em'} - \theta_{wg''}) + c_{ms''}(\dot{\theta}_{em'} - \dot{\theta}_{wg''}) + T_{cwg''}, \tag{3.11}$$

$$J_{em''}\ddot{\theta}_{em''} = T_{em''} - k_{ms''}(\theta_{em'} - \theta_{wg''}) - c_{ms''}(\dot{\theta}_{em'} - \dot{\theta}_{wg''}) - c_{em''}\dot{\theta}_{em''}, \tag{3.12}$$

$$m_{r''}\ddot{\chi}_{r''} = k_{r''}(C_f\theta_{ww''} - \chi_{r''}) - c_{r''}\dot{\chi}_{r''} - F_r. \tag{3.13}$$

The set of the RWA subsystem motion Eqs. (3.10)–(3.13) are presented for the SBW steering system model completeness. Besides Eq. (3.13), which is used in the comparison of the EPS and SBW system models, the corresponding equations are presented for reference.

3.3. Worm drive model, reaction torques $T_{cww} = T_{cww}(\theta_{wg}, \theta_{ww})$ and $T_{cwg} = T_{cwg}(\theta_{wg}, \theta_{ww})$

The worm drive contact model was published by Dohring *et al.* (1993). The reaction forces and reaction torques in the left-handed worm drive for the EPS system and the HWA subsystem were considered using the contact model shown in Fig. 3 published in (Tamura *et al.*, 2013) and further developed by Wilhelm *et al.* (2016). The stiffness of the contact points 1 and 2 of the worm and the worm wheel teeth is k_c. The equations of motion of the worm and the worm wheel about their respective axes of motion: x for the worm and y for the worm wheel, are presented in Fig. 3:

$$m_{wg}\ddot{x} = F^x_{cwg} = N_{2,wg}\sin\gamma\cos\beta - F_{f2,wg}\cos\gamma - N_{1,wg}\sin\gamma\cos\beta - F_{f1,wg}\cos\gamma, \tag{3.14}$$

$$m_{ww}\ddot{y} = F^y_{cww} = -N_{2,ww}\cos\gamma\cos\beta - F_{f2,ww}\sin\gamma + N_{1,ww}\cos\gamma\cos\beta - F_{f1,ww}\sin\gamma. \tag{3.15}$$

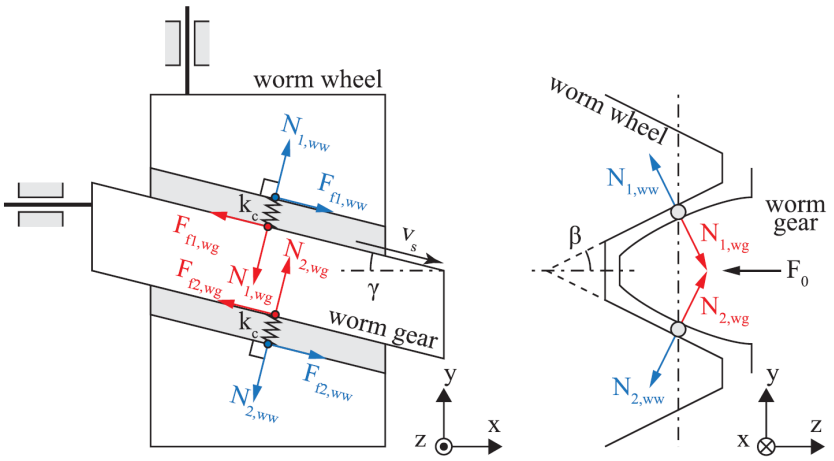

Fig. 3. Worm gear and worm wheel contact model (Wilhelm *et al.*, 2016).[1]

[1]Reprinted with permission from Wilhelm, F., Tamura, T., Fuchs, R., & Müllhaupt, P. (2016). Friction compensation control for power steering. *IEEE Transactions on Control Systems Technology*, © 2016 IEEE.

As shown in Fig. 3, the worm teeth are pressed against the worm wheel teeth by an initial pressure force F_0. As a result of the initial load, the contact points are precompressed by a distance h_0, which is described by Eq. (3.16):

$$h_0 = \frac{F_0}{2k_c \sin\beta}. \tag{3.16}$$

During motion, the elastic connection at the interaction points 1 and 2 of the worm gear and the worm wheel will undergo compression and decompression by a distance dh, which is described by Eq. (3.17). Compression by a distance dh of the elastic connection at contact 1 is equivalent to decompression at point 2, and vice versa. This dependence is included in the notation in the form of contact and normal forces presented in Eqs. (3.22) and (3.23) as a function of displacement dh where $\Delta\theta_{wg} = \Delta\theta_{wg}(t + \Delta t) - \theta_{wg}(t)$ and $\Delta\theta_{ww} = \Delta\theta_{ww}(t + \Delta t) - \theta_{ww}(t)$:

$$dh = r_{wg}\Delta\theta_{wg} \sin\gamma - r_{ww}\Delta\theta_{ww} \cos\gamma. \tag{3.17}$$

Normal forces in contact points:

$$N_{2,ww} = N_{2,wg} = k_c(\max(h_0 - dh, 0)), \tag{3.18}$$

$$N_{1,ww} = N_{1,wg} = k_c(\max(h_0 + dh, 0)). \tag{3.19}$$

Friction force:

$$\operatorname{sgn} v_{wg}\mu N_{2,ww} = F_{f2,ww} = F_{f2,wg}, \tag{3.20}$$

$$\operatorname{sgn} v_{wg}\mu N_{1,ww} = F_{f1,ww} = F_{f1,wg}. \tag{3.21}$$

Notation in the form of contact and normal forces as a function of displacement dh:

$$F_C(dh) = N_{1,ww} - N_{2,ww} = N_{1,wg} - N_{2,wg}, \tag{3.22}$$

$$F_N(dh) = N_{1,ww} + N_{2,ww} = N_{1,wg} + N_{2,wg}. \tag{3.23}$$

The equations of motion (3.14) and (3.15), after taking into account Eqs. (3.18)–(3.21), can be written using the contact and normal force representation as functions of dh, as presented by Wilhelm *et al.* (2016):

$$F^x_{cwg} = -F_C \sin\gamma \cos\beta - \operatorname{sgn} v_{wg}\mu F_N \cos\gamma, \tag{3.24}$$

$$F^y_{cww} = F_C \cos\gamma \cos\beta - \operatorname{sgn} v_{wg}\mu F_N \sin\gamma. \tag{3.25}$$

The friction coefficient in the EPS and SBW systems uses the model proposed by Rooney and Deravi (1982), in which the kinetic friction coefficient μ'_k is modeled by a hyperbolic tangent:

$$\mu'_k = \mu_{k_{\max}} \tanh C|\dot{x}|. \tag{3.26}$$

The meaning of the symbols in Eq. (3.26) is as follows: μ'_k is the equivalent coefficient of kinetic friction, $\mu_{k_{\max}}$ is the maximum coefficient of kinetic friction, $\dot{x}$ is the sliding velocity, C is a constant. The reaction torques T_{cwg} and T_{cww}, as published by Wilhelm *et al.* (2016), are defined by equations:

$$T_{cwg} = r_{wg}F^x_{cwg}, \tag{3.27}$$

$$T_{cww} = r_{ww}F^y_{cww}. \tag{3.28}$$

3.4. Comparison of the EPS system and the HWA subsystem

The conventional EPS system model shown in Fig. 1 differs from the communication bus-coupled SBW system model shown in Fig. 2 by the existence of a mechanical connection between the steering wheel and the road wheels. In mathematical models, this difference is represented by the expression $r_p C_f k_r(\theta_{ww} - \frac{\chi_r}{C_f})$ in Eq. (3.2). However, this component does not exist in the SBW system model. Equation (3.7) describing the HWA subsystem does not have this expression since there is no mechanical linkage between road wheels and the steering wheel. Equation (3.7) is equivalent to Eq. (3.2) from the EPS system model. Similarly, Eq. (3.13), which describes the RWA subsystem, is equivalent to Eq. (3.5) from the EPS system model. This element of the model constitutes the mechanical coupling between the steering rods and the steering wheel. The lack of direct impact of the force in the rods F_r on the steering wheel is ensured in the SBW steering system, which provides this information digitally via a communication bus, in order to generate feedback torque on the steering wheel for the driver. The models differ in the number of degrees of freedom. In total, EPS has five, while SBW has eight. Additionally, they partially differ in the scope of the functions they perform in the automotive vehicle. The most important functionality of sensing the driver's intentions regarding the vehicle's driving direction is exactly the same in the EPS and the HWA systems. In the EPS system, the desired steering angle is transmitted via a mechanical linkage. In the HWA subsystem of the SBW system, information about the desired steering angle is transmitted digitally by its ECU microprocessor via a communication bus to the microprocessor of the RWA subsystem ECU in the SBW system. An example of a functional difference between the EPS system and the HWA subsystem is the assistance function, which helps overcome resistance. This function is present in the EPS system, resulting, among other things, from the direct mechanical connection between the steering wheel and the road via tires, linkages, the steering rack, and other connecting elements. The HWA subsystem does not have a direct connection to the road; therefore, the resistance felt on the steering wheel in the EPS system does not occur in the HWA subsystem. The HWA subsystem generates a resistance torque for the driver, stiffening the steering wheel so that the driver can feel the steering system interacting with the road and the vehicle's behavior.

4. An experimental determination of the equivalent driving torque

An experiment to determine the equivalent electric motor driving torque for the HWA is divided into two stages: a and b. During stage a of the experiment, the angular displacements of the joint positions in the reference model (EPS system) are determined at a given electric motor driving torque $T^a_{em}(t)$. Stage b of the experiment uses the iterative execution of the multiple fourth-order Runge–Kutta method (RK4) integrations to find whether any of the results satisfies the given criteria, i.e., Eq. (4.1). Stage b of the experiment determines the family of driving torques $[T^b_{em'}]$, which is represented by a matrix with the number of rows equal to the number of time samples i and the number of columns equal to the number of evaluated driving torque amplitudes j. The matrix of the driving torque family is associated with the matrix of steering wheel angular displacement trajectories $[\theta^b_{sw'}(t)]$, where each row corresponds to a time sample and each column corresponds to an experimental result obtained for a particular driving torque from the family $T^b_{em'}(t)(j)$, i.e., $[\theta^b_{sw'}] = [\theta^b_{sw'}]([T^b_{em'}])$. The final driving torque is the one from the family $[T^b_{em'}]$ for which the associated angular displacement trajectory at the time of the steady state (time interval equal to five time constants) meets the given error criteria or yields a better result as per Eq. (4.1). For each experiment, the rack force $F_r = 0\,[\mathrm{N}]$ and the driver's torque $T_{dr} = 0\,[\mathrm{Nm}]$ will not affect the EPS system and the HWA subsystem.

$$Q(x) = \delta_{\theta_{sw\mathrm{Av}}} = f(T_{em'_{\mathrm{Amp}}}) \to \min \leq 5\,\%, \tag{4.1}$$

$$\delta_i = \left| \frac{\theta^b_{sw'}(i) - \theta^a_{sw}(i)}{\theta^a_{sw}(i)} \right| \cdot 100\,\%, \tag{4.2}$$

$$\delta = \frac{1}{n} \sum_{0}^{n} \delta_i, \tag{4.3}$$

$$\delta_{\theta_{sw\mathrm{Av}}} = \frac{1}{n} \sum_{0}^{n} \left| \frac{\theta^b_{sw'}(i) - \theta^a_{sw}(i)}{\theta^a_{sw}(i)} \right| \cdot 100\,\%. \tag{4.4}$$

The formulas are for the relative momentary error – Eq. (4.2), the general representation of the average relative error – Eq. (4.3), and the mean relative error of the angular position θ^b_{sw} – Eq. (4.4). In this study, the reference model is the EPS system. The driving torque T_{em} available on the electric motor's shaft is used as an input signal during simulations. The examined systems are excited by driving torques: T^a_{em} for the EPS system and $[T^b_{em'}]$ for the HWA. All driving torques are shaped as a pulse during analysis and their general form is defined by Eq. (4.5). The excitation driving torques T^a_{em} and $[T^b_{em'}]$ are defined as pulses lasting $\tau = 125\,\mathrm{ms}$. The input signals $T^a_{em}(t)$, $[T^b_{em'}(t)]$ are used to excite the examined systems into accelerated motion while driving and to allow the examined systems to settle on the final position in the steady states. During the simulation, a special case is examined in which all corresponding parameters are assumed to be the same for the EPS system and the HWA subsystem, i.e., $J_{em'} = J_{em}$, $J_{wg'} = J_{wg}$, $J_{ww'} = J_{ww}$, $J_{sw'} = J_{sw}$, $k_{ms'} = k_{ms}$, $k_{tb'} = k_{tb}$, $c_{em'} = c_{em}$, $c_{ms'} = c_{ms}$, $c_{sw'} = c_{sw}$. The individual transient driving torques $T^b_{em'}(t)(j)$ are described by Eq. (4.6), where j denotes the index of the element of the driving torque family $T^b_{em'}(t)$. During the experiment, the amplitude will belong to the interval $T^b_{em'}(t)(j) \in [0, T_{\max}]$:

$$T^a_{em}(t) = T_{\max} \cdot (1(t) - 1(t-\tau)), \tag{4.5}$$

$$T^b_{em'}(t)(j) = T^b_{\max'}(j) \cdot (1(t) - 1(t-\tau)). \tag{4.6}$$

The reference driving torque is defined by Eq. (4.5), where $\tau = 125\,\mathrm{ms}$. The target driving torques for the HWA subsystem of a family $[\theta^b_{sw'}(t)]$ are derived iteratively. Table 1 presents the selected driving torque amplitudes $T_{em'}(j)^b(t)$ and the results for the mean relative steering wheel angular position errors $\theta_{sw'}(j)^b(t)$.

Table 1. List of selected amplitudes of $T^b_{em'}(t)$ with their corresponding mean relative position errors $\theta^b_{sw'}(t)$.

Index	$T_{em'_{\mathrm{Amp}}}$	$\delta_{\theta_{sw\mathrm{Av}}}$
0	0	96.688
1	0.40704	96.688
2	0.42965	92.303
3	1.0176	69.422
4	1.5151	54.543
5	2.0126	39.854
6	2.5101	25.229
7	3.0075	10.648
8	**3.2769**	**4.568**
9	3.3026	4.605
10	3.505	6.718
11	4.0025	18.556
12	4.5	32.827

Figure 4a presents the reference driving torque for the EPS system $T^a_{em}(t)$ and selected driving torques for the family of driving torques for the HWA subsystem $[T^b_{em'}(t)]$, respectively indexed as: 0, 8, 11 from Table 1. The reference driving torque $T^a_{em}(t)$ is marked with a green line. The selected driving torques from the family $[T^b_{em}(t)]$ are marked as follows: $T^b_{em'}(t)(0) \rightarrow$ magenta line, $T^b_{em'}(t)(8) \rightarrow$ red line, $T^b_{em'}(t)(11) \rightarrow$ blue line. The driving torque $T^b_{em'}(t)(0)$ is deliberately equal to 0 because it verifies that the model of the system will not start motion unless it is externally driven. This is confirmed by ensuring that all of joint angular displacements: $\theta^b_{sw'}(t)(0)$, $\theta^b_{ww'}(t)(0)$, $\theta^b_{wg'}(t)(0)$, $\theta^b_{em'}(t)(0)$ are equal to 0. Figure 4b presents the reference angular position $\theta^a_{sw}(t) \rightarrow$ red line related to the reference driving torque $T^a_{em}(t)$ and the obtained angular positions: $\theta^b_{sw'}(t)(0) \rightarrow$ the magenta line, $\theta^b_{sw'}(t)(8) \rightarrow$ red line, $\theta^b_{sw'}(t)(11) \rightarrow$ blue line.

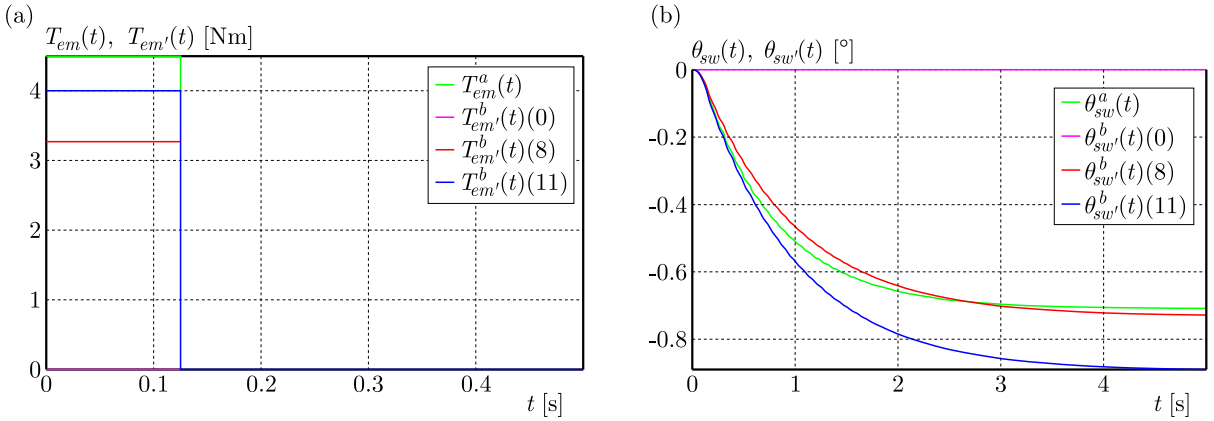

Fig. 4. (a) Driving torques $T_{em}(t)$, $T_{em'}(t)$; (b) angular displacements of the steering wheel $\theta_{sw}(t)$, $\theta_{sw'}(t)$ (normalized).

The indexes of the angular positions $0, 8, 11$ correspond to the driving torque amplitudes as shown in Table 1 and as they are presented in Fig. 4a. Table 1 presents the key results from hundreds of numerical calculations performed by the authors. The examined HWA subsystem model time constant for the steering wheel angular position as a function of the driving torque $\theta_{sw'} = \theta_{sw'}(T_{em'})$ is equal to $\tau_{\text{HWA}} = 0.983$ [s]. The τ_{HWA} was determined from the measurements as a time when the HWA system achieves its steering wheel angular position $\theta^b_{sw'}(t)(8)$ equal to 62.31 % of the target position in the steady state $\theta^b_{sw'}(t = 5\tau_{\text{HWA}})(8)$. The best results considering the steering wheel position in a steady state are obtained for $\theta^b_{sw'}(t)(8)$, which is affected by the mean relative error $\delta_{\theta_{sw\text{Av}}}(8)$ at the level of 4.568 %, comparing to the reference angular position trace $\theta^a_{sw}(t)$. The index 0, by means of $\theta^b_{sw'}(t)(0)$, verifies the model by confirming that it is not in motion for a driving torque equal to $0 \rightarrow T^b_{em'}(t)(0)$. The $\theta^b_{sw'}(t)(12)$ which is related to the driving torque $T^b_{em'}(t)(12) = T^a_{em}(t)$ is affected by the mean relative error $\delta_{\theta_{sw\text{Av}}}(12)$ at the level of 32.827 %. Figure 5 presents the momentary relative error of the steering wheel angular position $\delta\theta^b_{sw'}(t)(8)$ for the HWA subsystem which is obtained for $T^b_{em'}(t)(8)$ from Table 1. As a result of stages a and b, the driving torque amplitude for the HWA subsystem was obtained, which lies within the assumed permissible error of the objective function $Q(x)$ defined by Eq. (4.1). The smallest mean relative error $\delta_{\theta_{sw\text{Av}_{\min}}} = 4.568$ % was obtained for the driving torque amplitude $T_{em'_{\text{Amp}}} = 3.2769$ Nm. The final driving torque will be denoted as $T^c_{em'}(t) = T^b_{em'}(t)(j = j_{\min})$:

$$T^c_{em'}(t) = T_{\max'} \cdot (1(t) - 1(t - \tau)), \tag{4.7}$$

$$T^c_{em'}(t) = 3.2769 \cdot (1(t) - 1(t - 0.125)). \tag{4.8}$$

The work was focused on the strategy to determine a driving torque considering the trajectory in the time interval until the target steering wheel angular position is obtained, i.e., the

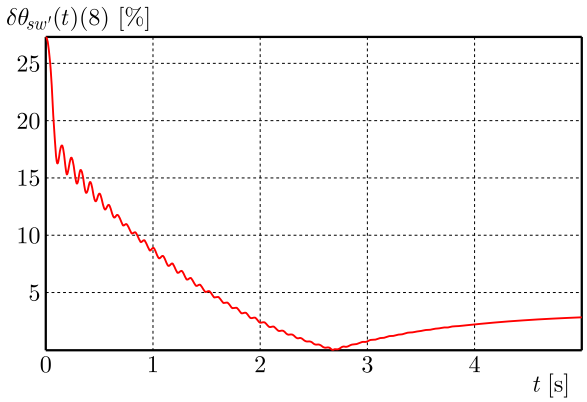

Fig. 5. Momentary relative error [%] of angular displacement for $\theta^{b}_{sw'}(t)(8)$ in the time interval until the steady state.

steady state is achieved. Figure 6 presents the trace of the momentary relative error for the angular position $\delta\theta^{b}_{sw'}(t)(8)$. When it comes to the time interval when the HWA is excited by the electric motor's driving torque, the mean momentary relative error $\delta\theta_{sw\mathrm{Av}}(8)_{t=125\,\mathrm{ms}} = 21.8\,\% \in [0\,\mathrm{ms}, 125\,\mathrm{ms}]$. Considering the $\theta^{b}_{sw'}(t)(8)$ trajectory in the excitation time interval $t_{\mathrm{exc}} \in [0\,\mathrm{ms}, 125\,\mathrm{ms}]$, in the transient state phase, the electric motor driving torque for the HWA direct scaling from the reference EPS requires a different strategy.

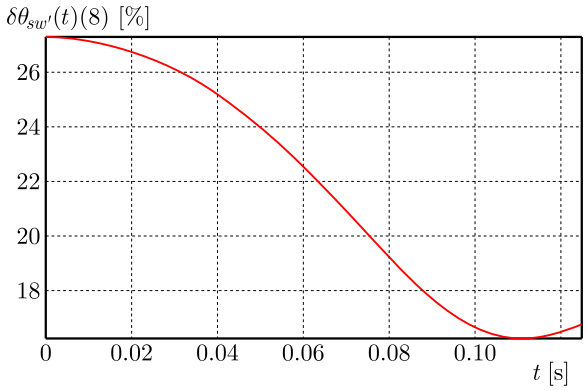

Fig. 6. Momentary relative error [%] of angular displacement for $\theta^{b}_{sw'}(t)(8)$ during the HWA excitation by its electric motor's driving torque $T^{b}_{em'}(t)(8)$.

5. Summary

The empirically obtained data allows the authors to formulate a coefficient which scales the amplitude of the driving torque from the EPS system to the HWA subsystem s_{EPS2HWA^*}, thus ensuring that the trajectory of the HWA steering wheel angular displacement falls within the range of the predefined mean relative error as per Eq. (4.4) in the time interval required to achieve the steady state, and fulfilling the criteria defined by Eq. (4.1):

$$s_{\mathrm{EPS2HWA}^*} = \frac{T_{em_{\mathrm{AmpHWA}}}}{T_{em_{\mathrm{AmpEPS}}}} = \frac{3.2769}{4.5} = 0.7282. \tag{5.1}$$

The scaling coefficient s_{EPS2HWA^*}, which is defined by Eq. (5.1), transforms the amplitude of a pulse shaped reference electric motor driving torque. The coefficient s_{EPS2HWA^*} allows a command to be scaled from a projected motor torque curve from the EPS system to a HWA subsystem. The linear scaling coefficient can be applied in microprocessor embedded systems in various automotive ECUs. Its impact on the computational capability and the microcontroller

resources is low and can be performed in real time. Applying the scaling factor from Eq. (5.1) of the HWA subsystem electric motor driving torque can be defined by Eq. (5.2):

$$T_{em'}(t) = s_{\text{EPS2HWA}^*} \cdot T_{em}(t). \tag{5.2}$$

The results were obtained for a specific case where all of the corresponding constant parameters of the EPS system and the HWA subsystem were assumed as equal (Subsection 3.4). Further research is focused on determining a scaling coefficient which is dependent on multiple parameter relations:

$$s_{\text{EPS2HWA}} = s_{\text{EPS2HWA}}\left(\frac{T_{em'}}{T_{em}}, \frac{J_{em'}}{J_{em}}, \frac{J_{wg'}}{J_{wg}}, \frac{J_{ww'}}{J_{ww}}, \frac{J_{sw'}}{J_{sw}}, \frac{k_{ms'}}{k_{ms}}, \frac{k_{tb'}}{k_{tb}}, \frac{c_{em'}}{c_{em}}, \frac{c_{ms'}}{c_{ms}}, \frac{c_{sw'}}{c_{sw}}\right). \tag{5.3}$$

Based on the analysis of the obtained traces, it is concluded that the proposed model of the HWA subsystem of the SBW system, in terms of shape, reflects the conventional EPS system steering wheel angular position trajectory with good approximation in the time interval ending in steady state. Additionally, limitations of the driving torque scaling strategy were observed during the system excitation interval, which constitutes a direction for further research.

References

1. Badawy, A., Zuraski, J., Bolourchi, F., & Chandy, A. (1999). Modeling and analysis of an electric power steering system. *SAE Technical Papers*. https://doi.org/10.4271/1999-01-0399
2. Canudas-de-Wit, C., Bechart, H., Claeys, X., Dolcini, P., & Martinez, J.-J. (2005). Fun-to-drive by feedback. *European Journal of Control*, *11*(4–5), 353–383. https://doi.org/10.1016/s0947-3580(05)71042-6
3. Chen, H., Yang, Y., & Zhang, R. (2011). Study on Electric Power Steering system based on ADAMS. *Procedia Engineering*, *15*, 474–478. https://doi.org/10.1016/j.proeng.2011.08.090
4. Ciarla, V., Cahouet, V., Canudas De Wit, C., & Quaine, F. (2012). Genesis of booster curves in Electric Power Assistance Steering systems. In *2012 15th International IEEE Conference on Intelligent Transportation Systems* (pp. 1345–1350). IEEE. https://doi.org/10.1109/ITSC.2012.6338807
5. Dilger, E., Ahner, P., Lohner, H., Dominke, P., Cao, C.-T., Nguyen, N.-T., Janetzke, H., Allgeier, T., Pfeiffer, W., Yuan, B., Muller, B., Ries-Mueller, K., Harter, W., Sauer, T., Hess, W., & Blessing, P. (2001). S*teer-by-wire steering system for motorized vehicles* (U.S. Patent No. 6219604B1). U.S. Patent and Trademark Office. http://www.google.com/patents/US6219604
6. Dohring, M.E., Lee, E., & Newman, W.S. (1993). A load-dependent transmission friction model: theory and experiments. In *[1993] Proceedings IEEE International Conference on Robotics and Automation*, Vol. 3 (pp. 430–436). IEEE. https://doi.org/10.1109/robot.1993.292210
7. Dominke, P., Cao, C.-T., Pfeiffer, W., Yuan, B., Leimbach, K.-D., Mueller, B., Harter, W., Blessing, P., Schuele, J., & Lohner, H. (2002). *Method for controlling a steer-by-wire system* (U.S. Patent No. 6871127B2). U.S. Patent and Trademark Office. https://patents.google.com/patent/US6871127B2/en?oq=US+6%2C871%2C127
8. Eickholt, M.A., Golda, F.N., Kern, P.E., Marr, J.L., Otto, J.M., & Stilwell, E.N. (2019). *Road wheel actuator assembly* (U.S. Patent No. 10322744B2). U.S. Patent and Trademark Office. http://www.google.com/patents/US10322744
9. Feick, S., Pandit, M., Zimmer, M., & Uhler, R. (2000). Steer-by-wire as a mechatronic implementation. *SAE Technical Papers*, *109*, 1152–1160. https://doi.org/10.4271/2000-01-0823
10. Führer, T., & Schedl, A. (1999). The steer-by-wire prototype implementation: Realizing time triggered system design, fail silence behavior and active replication with fault-tolerance support. *SAE Technical Papers*. https://doi.org/10.4271/1999-01-0400
11. Guan, X., Zhang, Y.N., Lu, P.P., Duan, C.G., & Zhan, J. (2024). The control strategy of the electric power steering system for steering feel control. *Proceedings of the Institution of Mechanical Engineers, Part D: Journal of Automobile Engineering*, *238*(2–3), 347–357. https://doi.org/10.1177/09544070221132131

12. Haas, A., Menze, G., Sieberg, P. M., & Schramm, D. (2023). An objective evaluation approach for safety-relevant steering feedback on a test bench. *Vehicles*, *5*(4), 1727–1742. https://doi.org/10.3390/vehicles5040094

13. Han, Y., He, L., Wang, X., & Zong, C. (2014). Research on torque ratio based on the steering wheel torque characteristic for steer-by-wire system. *Journal of Applied Mathematics*, *2014*(1), Article 929164. https://doi.org/10.1155/2014/929164

14. Hu, T.-H., Yeh, C.-J., Ho, S.-R., Hsu, T.-H., & Lin, M.-C. (2008). Design of control logic and compensation strategy for electric power steering systems. In *2008 IEEE Vehicle Power and Propulsion Conference (VPPC)*. IEEE. https://doi.org/10.1109/VPPC.2008.4677471

15. Jang, B., Lee, D., Kim, K., & Kim, K.-S. (2022). Road torque modeling for electric power steering systems. *International Journal of Automotive Technology*, *23*(3), 765–773. https://doi.org/10.1007/s12239-022-0068-0

16. Kazemi, R., & Mousavinejad, I. (2011). A Comprehensive model for developing of Steer-By-Wire System. *International Journal of Mechanical, Industrial and Aerospace Sciences*, *5*(8), 1688–1694. https://scholarly.org/pdf/display/a-comprehensive-model-for-developing-of-steer-by-wire-system

17. Kuranowski, A. (2019). Electrical power steering – modelling and bench testing. *Technical Transactions*, *8*(116), 143–158. https://doi.org/10.4467/2353737xct.19.085.10864

18. Li, Q., & He, R. (2005). Modeling and simulation study of the steer by wire system using bond graph. *2005 IEEE International Conference on Vehicular Electronics and Safety* (pp. 7–11). IEEE. https://doi.org/10.1109/ICVES.2005.1563604

19. Magnus, B.J., Augustine, M.J., & Cole, M.J. (2002). *Steer-by wire handwheel actuator* (U.S. Patent No. 0189888A1). U.S. Patent and Trademark Office. https://patents.google.com/patent/US20020189888A1/en

20. Manca, R., Circosta, S., Khan, I., Feraco, S., Luciani, S., Amati, N., Bonfitto, A., & Galluzzi, R. (2021). Performance assessment of an electric power steering system for driverless formula student vehicles. *Actuators*, *10*(7), Article 165. https://doi.org/10.3390/act10070165

21. Menjak, R., Haupt, J., Card, J.M., & Thomas, S.M. (2004). *Hand wheel actuator* (U.S. Patent No. 6799654B2). U.S. Patent and Trademark Office. http://www.google.com/patents/US6799654

22. Mirmohammad Sadeghi, S.H., Sesana, R., & Maffiodo, D. (2017). Friction calculation and simulation of column electric power steering system. *International Journal of Mechanical and Mechatronics Engineering*, *11*(1), 153–160. https://doi.org/10.5281/zenodo.1339980

23. Nguyen, T.A. (2025). Mathematical modeling and characteristics of automotive electric power steering systems: A state–of–the–art literature review. *Ain Shams Engineering Journal*, *16*(9), Article 103516. https://doi.org/10.1016/j.asej.2025.103516

24. Nidec Corporation, *Automotive EPS*. Retrieved February 7, 2025, from https://www.nidec.com/en/product/search/category/ B101/M102/S100/NCJ-Automotive-EPS-02/.

25. Perdana, M.A.P., Budiman, A.C., Ristiana, R., Muharam, A., Ismail, K., Kurnia, M.R., Amin, Huda, N., Kaleg, S., & Hapid, A. (2025). Control strategies for steer-by-wire systems: An overview. *Technologies*, *13*(1), Article 6. https://doi.org/10.3390/technologies13010006

26. Pfeffer, P.E., Harrer, M., & Johnston, D.N. (2008). Interaction of vehicle and steering system regarding on-centre handling. *Vehicle System Dynamics*, *46*(5), 413–428. https://doi.org/10.1080/00423110701416519

27. Polmans, K. (2016). *Steer-by-wire steering system with couplable single-wheel steering systems* (German Patent No. WO2017198549A1). German Trademark and Patent Office. https://patents.google.com/patent/WO2017198549A1/en

28. Rooney, G.T., & Deravi, P. (1982). Coulomb friction in mechanism sliding joints. *Mechanism and Machine Theory*, *17*(3), 207–211. https://doi.org/10.1016/0094-114X(82)90006-4

29. Shimizu, Y., & Kawai, T. (1991). Development of electric power steering. *SAE Technical Papers*. https://doi.org/10.4271/910014

30. Tamura, T., Maroonian, A., Higashi, M., & Fuchs, R. (2013). Modeling and simulation for dynamic analysis of column type electric power steering. *JTEKT Engineering Journal*, *1010*(1010E), 19–25. https://www.jtekt.co.jp/e/engineering-journal/assets/1010/1010e_05.pdf

31. Tavoosi, V., Kazemi, R., & Hosseini, S.M. (2014). Vehicle handling improvement with steer-by-wire system using hardware in the loop method. *Journal of Applied Research and Technology*, *12*(4), 769–781. https://doi.org/10.1016/S1665-6423(14)70093-8

32. Wilhelm, F., Tamura, T., Fuchs, R., & Müllhaupt, P. (2016). Friction compensation control for power steering. *IEEE Transactions on Control Systems Technology*, *24*(4), 1354–1367. https://doi.org/10.1109/TCST.2015.2483561

33. Yih, P. (2005). *Steer-by-wire: Implications for vehicle handling and safety* [doctoral dissertation, Stanford University]. Stanford University, Dynamic Design Lab. https://ddl.stanford.edu/publications/thesis/steer-wire-implications-vehicle-handling-and-safety

34. Yih, P., & Gerdes, J. (2004). Steer-by-wire for vehicle state estimation and control. *Proceedings of AVEC*, 785–790. http://www-cdr.stanford.edu/dynamic/bywire/avec2004_v2.pdf

35. Yin, H., Wang, Z., Liu, J., & Liu, P. (2024). Steer-by-wire control algorithm using a dual-layer closed-loop model. *Scientific Reports*, *14*, Article 28536. https://doi.org/10.1038/s41598-024-79703-6

Manuscript received October 25, 2025; accepted for publication May 4, 2026;
published online June 20, 2026.